Supporting Information

Label-free detection of *Staphylococcus aureus* based on bacteria-imprinted polymer and turn-on fluorescence probes

Yuanyuan Guo, Juan Li*, Xiuling Song, Kun Xu, Juan Wang,* and Chao Zhao

School of Public Health, Jilin University, Changchun 130021, China

*Corresponding authors: email: li_juan@jlu.edu.cn TeL: 86-13664319729, jwang0723@jlu.edu.cn TeL: 86-13194376570

1. Synthesis of gold nanoparticles (AuNPs)

The well-dispersed AuNPs were directly synthesized via sodium citrate reduction method described in our previous report [1]. In a typical experiment, 2.5 mL of a $HAuCl_4 \cdot 3H_2O$ solution (0.2% w/v) in 50 mL of distilled water were heated to boiling, and then 2 mL of sodium-citrate solution (1% w/v, containing 0.05% w/v citric acid) were added quickly to the vigorously stirred solution. After further refluxing for 5 min, the mixture was allowed to cool down to ambient temperature. The resultant citrate-stabilized AuNPs colloids were stored at 4 °C.

2. **Table S1.** Zeta potential of different kind of bacteria

bacteria	**Zeta Potential (mv)**
S. aureus	-46.04
K. pneumoniae	-34.96
L. monocytogenes	-38.17
E. coli O157:H7	-10.61
S. typhimurium	-18.38
V. Parahaemolyticus	-30.96
S. Bogdi	-20.96

3. **Table S2.** Zeta potential of CA-CuNCs with different amount of citric acid carried

CA (mg)	Zeta Potential (mv)
6.8	9.26
10	5.87
20	-4.42
30	-12.17
40	-23.06
50	-36.31
60	**-43.92**
70	-44.91

4. Feasibility study of sonication treatment

To verify whether *S. aureus* was still present on the imprinted membrane after template removal by sonication, the imprinted PDMS film was removed from the surface of slide with and without ultrasound treatment. Bacterial nucleic acid was extracted by boiling method, then PCR amplification was conducted, and the results were determined by agarose gel electrophoresis.

As shown in Figure S1, the electrophoretic band of the film (lane 1) without ultrasound treatment was obvious, indicating a large number of *S. aureus* existed on the films. However, after the ultrasound treatment, no bands appeared after electrophoresis (lane 2), which indicated that the ultrasound treatment could completely remove the *S. aureus* template.

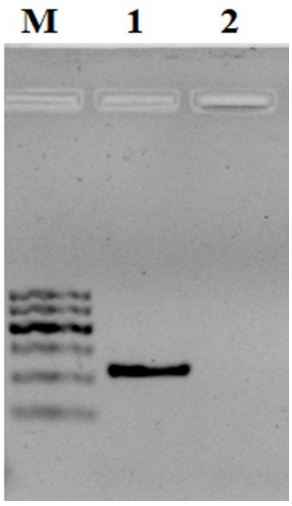

Figure S1. Result of agarose gel electrophoresis (M: marker; 1: BIPF without ultrasonic process; 2: BIPF with ultrasonic process).

5. Imprinted depth of the cavity of BIPF.

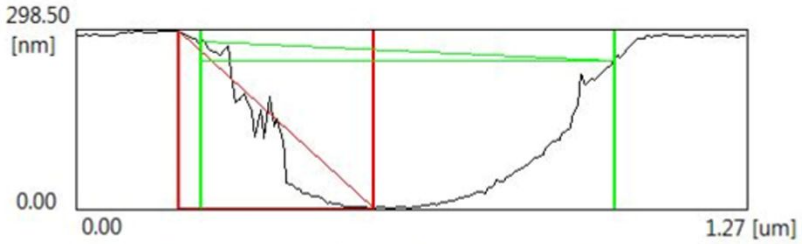

	Width[um]	Height[nm]	Angle[deg]
—	0.37	297.59	38.81
—	0.79	29.55	2.16

Figure S2. Imprinted depth of the cavity of BIPF.

6. Imprinted depth of the cavity of POTS-modified BIPF

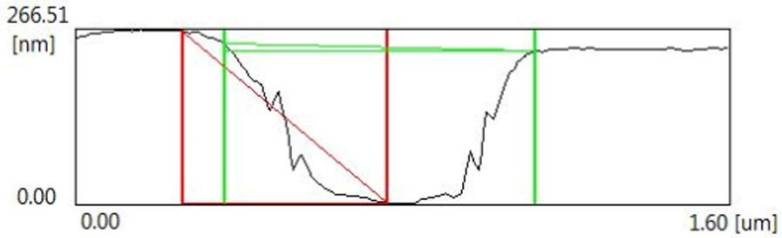

	Width[um]	Height[nm]	Angle[deg]
—	0.50	261.83	27.59
—	0.76	10.03	0.76

Figure S3. Imprinted depth of the cavity of POTS-modified BIPF.

7. POTS-modified BIPF incubated with *S. aureus*

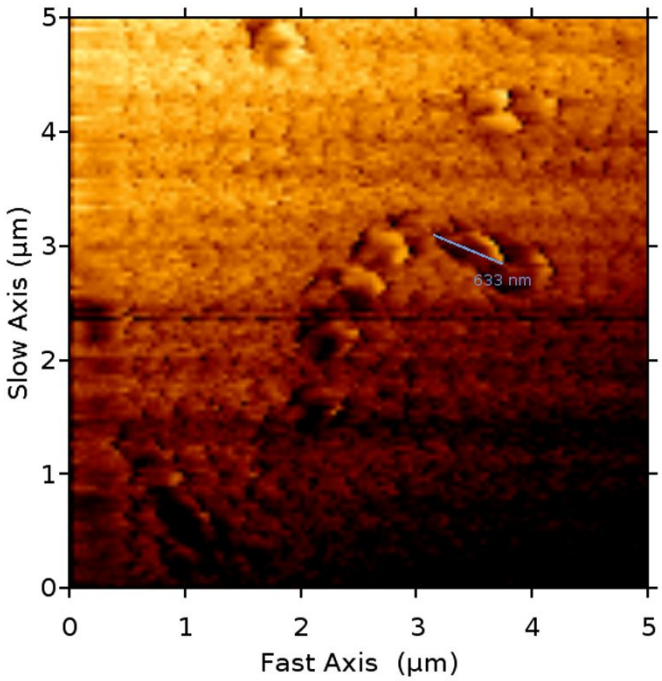

Figure S4. POTS-modified BIPF were filled after incubation with 10^5 cfu·mL^{-1} of *S. aureus* for 2 h.

8. **Table S3.** Dynamic contact Angles of PDMS films

Classification	Advance Angle	Back Angle	Lag Angle
NIPF	122.7555	99.3968	23.3587
POTS-modified NIPF	110.8186	105.2685	5.5501
BIPF	118.1535	87.4759	30.6776
POTS-modified BIPF	108.5472	102.5960	5.9512
POTS-modified BIPF+*S. aureus*	116.4275	99.3648	17.0627

9. Absorption efficiency of NIPF

The overnight cultured *S. aureus* was diluted with 0.01M PH 7.4 PBS to 10^6 cfu/mL with a total of 25 mL. After thoroughly mixed, 20 mL of the bacterial solution was co-incubated with NIPF for 2 h, and then transferred to a clean and sterilized 50 mL centrifuge tube. To avoid the occurrence of false adsorption, 5 mL 0.01M PBS was used to wash the surface of NIPF, and the washing process was repeated for three times. The resulting 15 mL washing solution was mixed with the above 20 mL bacterial solution, and its concentration (N) was determined by the plate counting method after 10-fold gradient dilution. As the negative control, 2 mL bacterial solution was added to 0.01M PBS to make up to 3.5 mL, and its concentration (N_0) was determined by plate counting method after 10-fold gradient dilution . The adsorption efficiency percentages were calculated based on the following equation:

$$\textbf{Absorption efficiency} = (\boldsymbol{N_0} - \boldsymbol{N})/\boldsymbol{N_0} \times 100\% \qquad (1)$$

The plate count results were shown in the Figure S5. According to equation (1)， the adsorption efficiency is 21.43 % (Table S4).

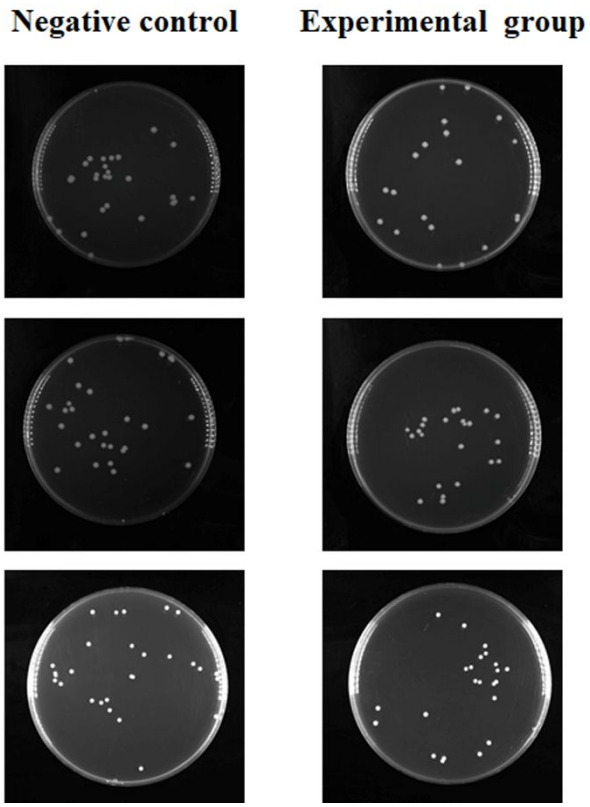

Figure S5. Plate count results of *S. aureus* before (left) and after (right) incubation with NIPF.

Table S4. Absorption quantity of NIPF on *S. aureus*

Initial bacterial quantity (N_0, cfu/mL)	Plate count results after incubation (N, cfu/mL)	Absorption quantity (%)
$2.45*10^{10}$	$1.93*10^{10}$	21.43

10. Capture rate evaluation

Set the amount of *S. aureus* that can be captured by a POTS-modified BIPF to be N.

The steps are as follows: POTS-modified BIPF was incubated with 10 mL $5*10^7$ cfu·mL^{-1} *S. aureus* (N_0) for 2 h. Then the supernatant was diluted 10-fold in a series and 200 μL of three different dilutions (10^{-5}, 10^{-6}, 10^{-7}) were taken for plate coating on the LB agar and cultured at 37 ℃ for 15 h [2]. The plate count results are shown in Table S5.

Table S5. Sensitivity of the Label-free detection method and other methods

concentration	10^{-5}	10^{-6}	10^{-7}
parallel sample 1	169	17	1
parallel sample 2	165	17	2
parallel sample 3	167	16	2
mean	167	16.67	1.67

According to Table S5, the mean amount of the three different dilutions (10^{-5}, 10^{-6}, 10^{-7}) were 167, 16.67 and 1.67, respectively. Combined with the volume of the obtained liquid, the amount of *S. aureus* in the supernatant after incubation (N_1) was calculated to be $8.35*10^7$ cfu.

$$\boldsymbol{N = N_0 - N_1} \quad (2)$$

$$\textbf{Adsorption efficiency} = (\boldsymbol{N_0 - N_1})/\boldsymbol{N_0} \times \mathbf{100}\% \qquad (3)$$

Therefore, the amount of *S. aureus* that can be captured by the POTS-modified BIPF prepared in this experiment is calculated as $4.165*10^8$ cfu and the adsorption efficiency is 83.3%.

11. **Table S6.** Adsorption efficiency of POTS-modified BIPF to different common foodborne pathogens

Material	bacteria	Initial amount (cfu /mL)	Plate count (cfu/mL)	Absorption efficiency (%)
POTS modified-BIPF	*S. aureus*	$9.45*10^8$	$1.31*10^8$	86.11
	E.coli O157:H7	$1.37*10^9$	$9.89*10^8$	27.56
	S. typhimurium	$1.75*10^9$	$1.31*10^9$	25.00
	K. pneumoniae	$1.31*10^9$	$1.05*10^9$	20.00
	S. boydii	$1.69*10^9$	$1.35*10^9$	20.21
	L. monocytogenes	$1.68*10^9$	$1.26*10^9$	25.00

Absorption efficiency(%)=(Initial amount-Plate count)/Initial amount*100%

12. The physical picture of the polymer films used in the experiment

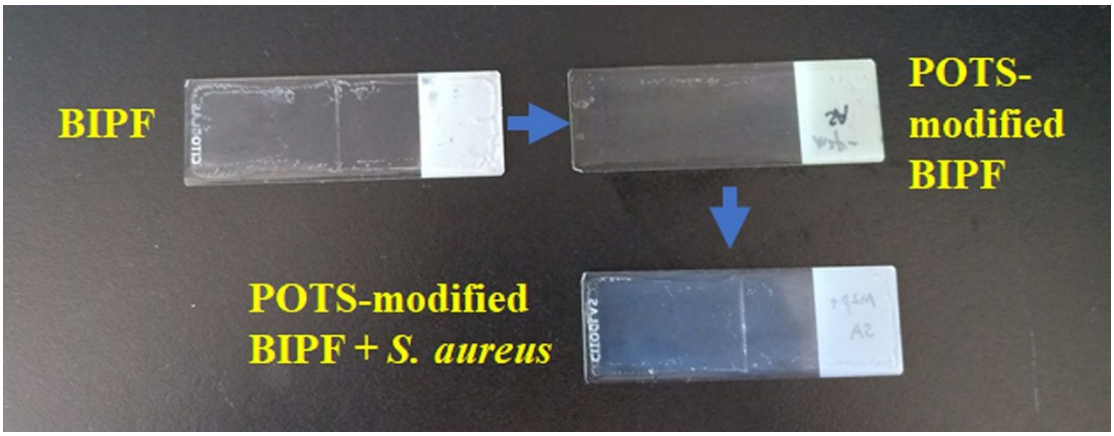

Figure S6. Pictures of BIPF, POTS-modified BIPF and POTS-modified BIPF incubated with *S. aureus* taken in natural light.

13. Characterization of AuNPs and DA-AuNPs

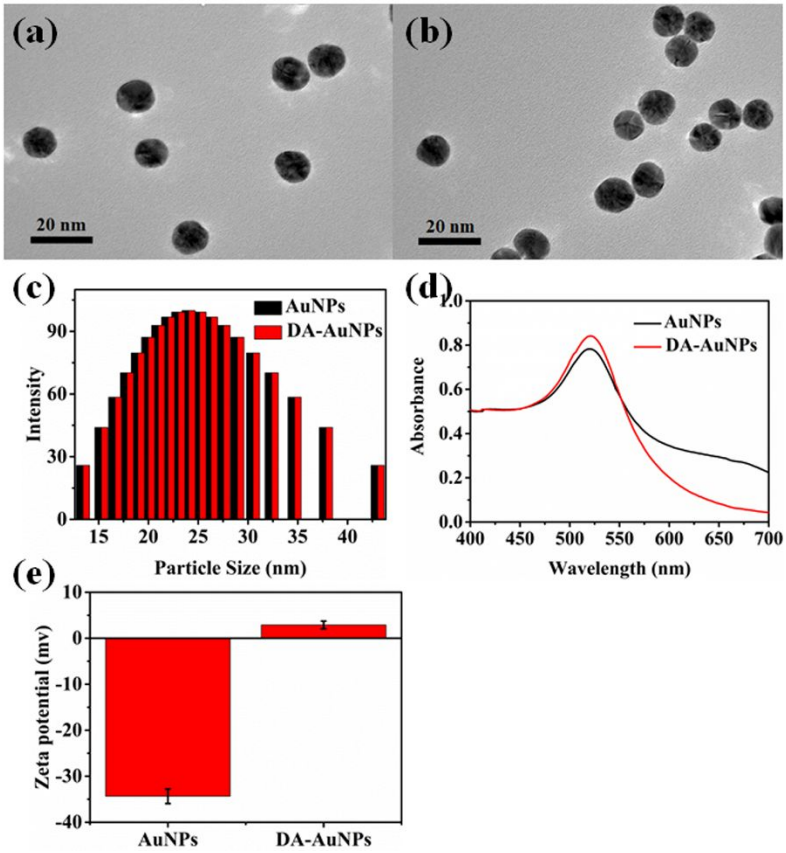

Figure S7. TEM images of (a) AuNPs and (b) DA-AuNPs. (c) Dynamic light scattering (DLS) spectrum of AuNPs and DA-AuNPs. (d) UV-Vis spectrum of AuNPs and DA-AuNPs. (e) Zeta potential of AuNPs and DA-AuNPs. Error bars represent the standard deviation of three replicates.

14. Characterization of CuNCs and CA-CuNCs

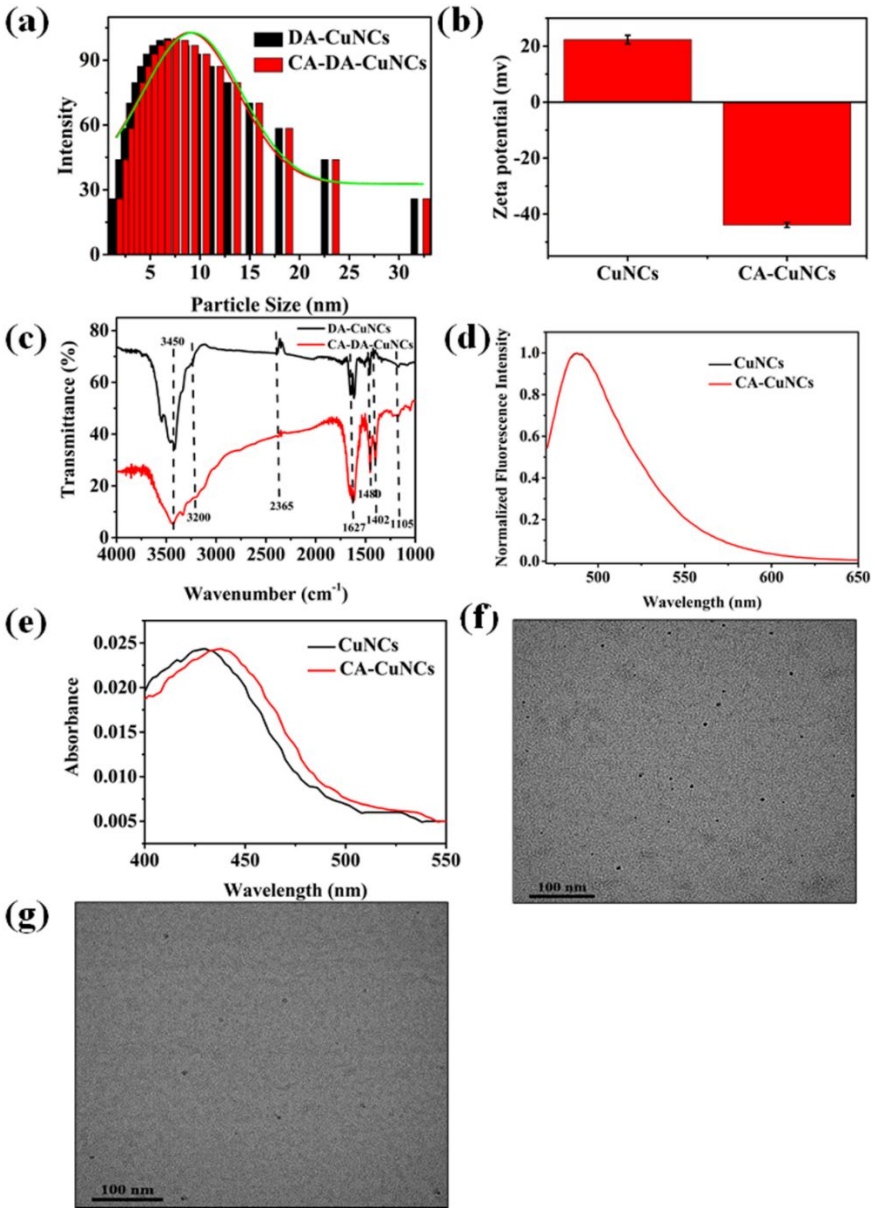

Figure S8. (a) Dynamic light scattering (DLS) spectrum of CuNCs and CA-CuNCs. (b) Zeta potential of CuNCs and CA-CuNCs. (c) FT-IR spectrum of CuNCs and CA-CuNCs. (d) Fluorescence and (e) UV spectrum of CuNCs and CA-CuNCs. TEM images of (f) CuNCs and (g) CA-CuNCs. Error bars represent the standard deviation of three replicates.

15. TEM image of CA-DA-CuNCs mixed with DA-AuNPs

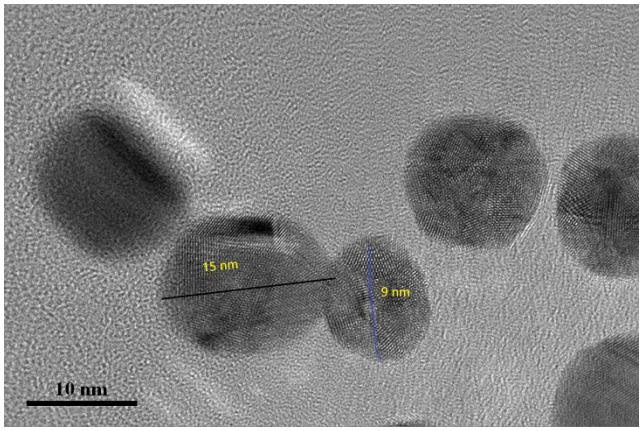

Figure S9. TEM image of CA-DA-CuNCs mixed with DA-AuNPs

16. The measurement of fluorescence lifetime

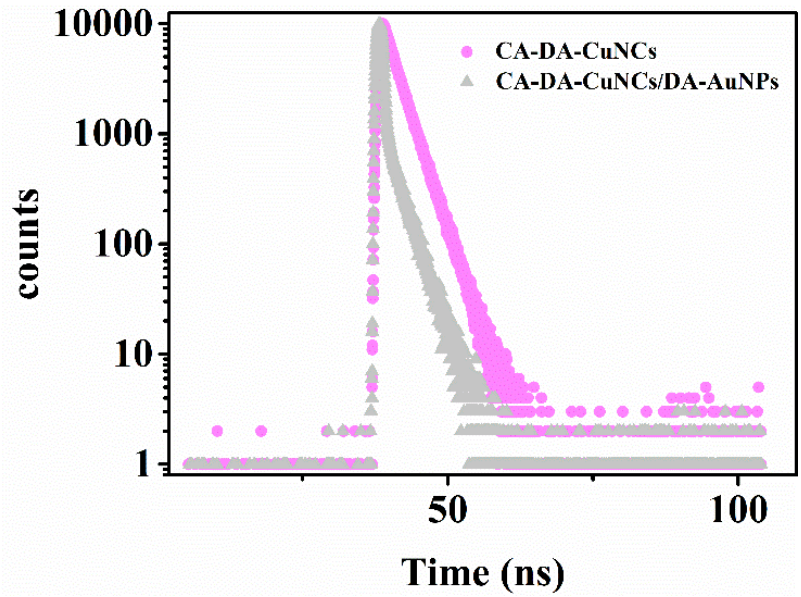

Figure S10. The fluorescence lifetime of CA-DA-CuNCs with/without DA-AuNPs.

Table S7. The fluorescence lifetime parameters of CA-DA-CuNCs with/without DA-AuNPs

Sample	T1	B1	T2	B2	Lifetime (ns)
CA-DA-CuNCs	1.732×10^{-9}	15.31%	2.712×10^{-9}	84.69%	2.50
CA-DA-CuNCs / DA-AuNPs	7.811×10^{-11}	79.57%	2.602×10^{-9}	20.43%	0.09

17. Optimization of the dosage of DA-AuNPs

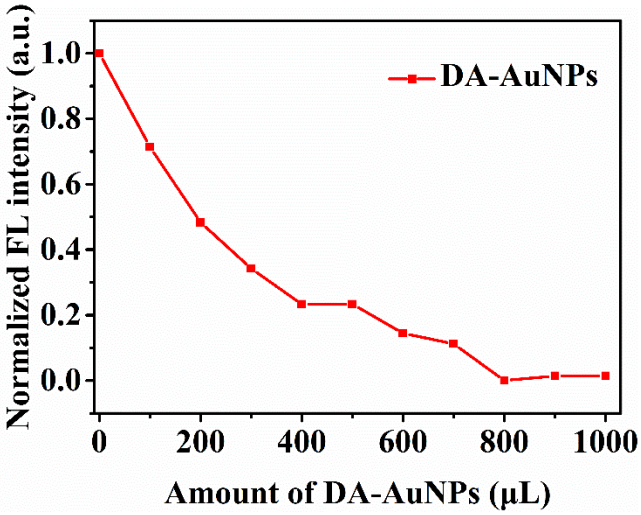

Figure S11. Fluorescence intensity of CA-DA-CuNCs with different amount of DA-AuNPs

18. Optimization of the incubation time

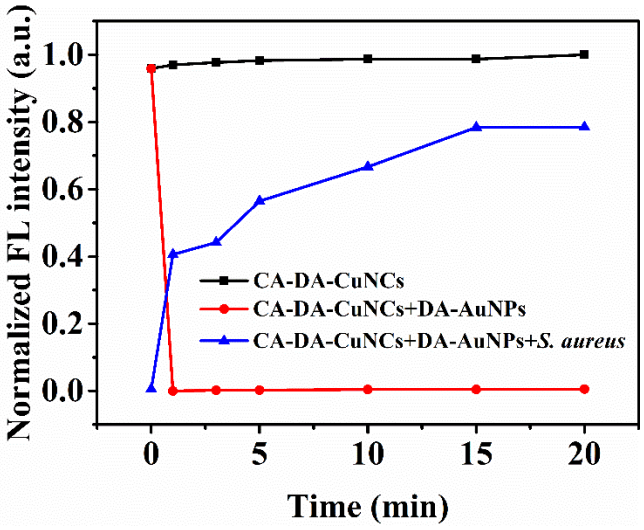

Figure S12. Optimization of the incubation time (0, 1, 3, 5, 10, 15, 20 min).

19. Original fluorescence spectrum of the specificity

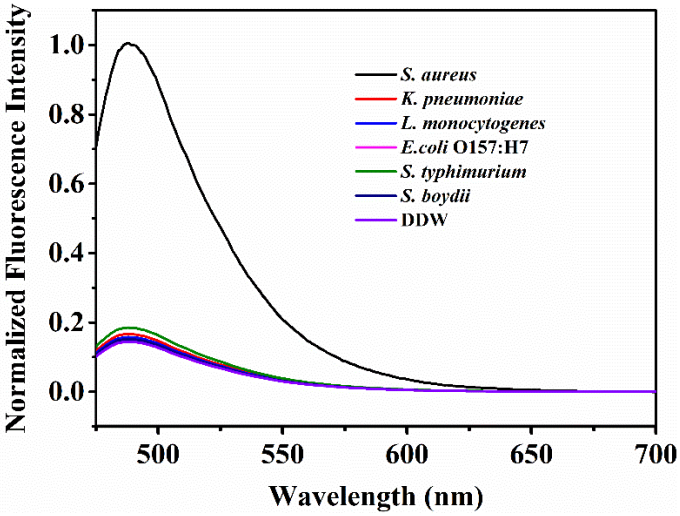

Figure S13. Normalized fluorescence intensity with different foodborne pathogens existed in the detection system.

20. Detection of *S. aureus* in real samples

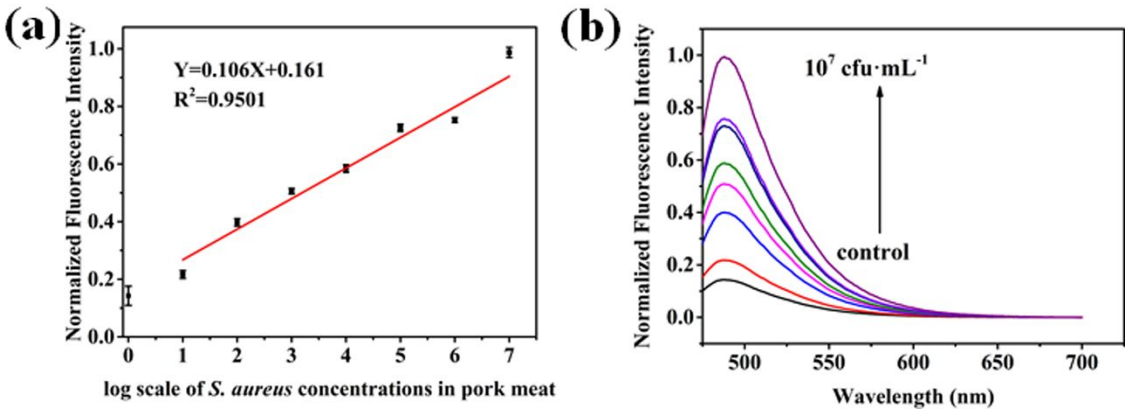

Figure S14. (a) Normalized fluorescence intensity with different concentrations of *S. aureus* (0, 10, 10^2, 10^3, 10^4, 10^5, 10^6, and 10^7 cfu·mL^{-1}) in pork meat samples. (b) The calibration curve for *S. aureus* in pork meat samples. (Fluorescence intensity vs the logarithm of *S. aureus* concentration). Error bars represent the standard deviation of three replicates.

21. **Table S8.** Sensitivity of the Label-free detection method and other methods

Method	LOD
surface-enhanced Raman scattering imaging[3]	300 cfu·mL^{-1}
count-on-a-cartridge (coc)[4]	100 cfu/g
Colorimetric[5]	10^4 cfu·mL^{-1} (naked eye)
	10^2 cfu·mL^{-1} (spectrophotometry)
Conductometric sensor[6]	4.0×10^3 cfu·mL^{-1}
Label-free nanophotonic interferometric biosensor[7]	29 cfu·mL^{-1}
This method	11.12 cfu·mL^{-1}

References

(1) Liu, Y.; Zhao, C.; Fu, K.; Song, X.; Xu, K.; Wang, J.; Li, J. Selective turn-on fluorescence detection of Vibrio parahaemolyticus in food based on charge-transfer between CdSe/ZnS quantum dots and gold nanoparticles. *Food Control* **2017**, 80, 380-387.

(2) Fu, K.; Zhang, H.; Guo, Y.; Li, J.; Nie, H.; Song, X.; Xu, K.; Wang, J.; Zhao, C. Rapid and selective recognition of *Vibrio parahaemolyticus* assisted by perfluorinated alkoxysilane modified molecularly imprinted polymer film. *RSC Advances* **2020**, *10*(24), 14305-14312.

(3) He, J.; Qiao, Y.; Zhang, H.; Zhao, J.; Li, W.; Xie, T.; Zhong, D.; Wei, Q.; Hua, S.; Yu, Y.; Yao, K.; Santos, H. A.; Zhou, M. Gold–silver nanoshells promote wound healing from drug-resistant bacteria infection and enable monitoring via surface-enhanced Raman scattering imaging. *Biomaterials* **2020**, *234*, 119763.

(4) Lee, W. I.; Park, Y.; Shrivastava, S.; Jung, T.; Meeseepong, M.; Lee, J.; Jeon, B.; Yang, S.; Lee, N. E. A fully integrated bacterial pathogen detection system based on count-on-a-cartridge platform for rapid, ultrasensitive, highly accurate and culture-free assay. *Biosens Bioelectron* **2020**, *152*, 112007.

(5) Le, T. N.; Tran, T. D.; Kim, M. I. A Convenient Colorimetric Bacteria Detection Method Utilizing Chitosan-Coated Magnetic Nanoparticles. *Nanomaterials* **2020**, *10*(1), 92.

(6) Zhang, X.; Wang, X.; Yang, Q.; Jiang, X.; Li, Y.; Zhao, J.; Qu K. Conductometric sensor for viable *Escherichia coli* and *Staphylococcus aureus* based on magnetic analyte separation via aptamer. *Mikrochim Acta* **2019**, *187*(1), 43.

(7) Maldonado, J.; Estevez, M.-C.; Fernández Gavela, A.; Gonzalez-Lopez, J. J.; Gonzalez-Guerrero, A. B.; Lechuga, L. M. Label-free detection of nosocomial bacteria using a nanophotonic interferometric biosensor. *Analyst* **2019**, *145*(2), 497-506.